ALMA Memo 581

Selection of Walsh functions for ACA

Kamazaki, T., Okumura, S. K., Chikada, Y.
ALMA project office, National Astronomical Observatory of Japan,
2-21-1 Osawa Mitaka Tokyo 181-8588, Japan
kamazaki.takeshi@nao.ac.jp
2008-09-15

Abstract

ALMA system adopts Walsh functions of 128 patterns in length as 180-degree and 90-degree phase switching patterns. However, ACA can not freely choose patterns from them, because switching base time is required to be a multiple of FFT operation interval of ACA Correlator. In addition, the pattern length of 128 is not necessary, because there are only 16 antennas in the ACA. Thus, from the Walsh functions of 128 patterns, we searched ones which were available in the ACA. We also estimated sensitivity leakage, sensitivity loss and crosstalk power with 1% time shift of the Walsh functions. As a result of this study, sixteen Walsh functions with smaller sensitivity leakage and loss have been chosen as candidates for phase switching patterns for the ACA. With the selected functions, the sensitivity leakage and loss can achieve 2.5 % or less and 0 % in the case of 1 % time shift between modulation and demodulation of an identical Walsh function, respectively. The averaged sensitivity leakage and loss over the combination of two Walsh functions are 1.3 % or less and 1.3 % or less in the same case, respectively. The RSS crosstalk power can achieve 1.2 % or less in the case of 1% time shift between two different Walsh functions, respectively.

1. Specifications of phase switching in ALMA

The ALMA system adopts 180-degree phase switching for bias and spurious cancellation and 90-degree phase switching for sideband rejection and sideband separation. Walsh functions are used as patterns of these phase switching (Emerson 2005; hereafter MEMO537). The specifications of the switching patterns follow:

- ♦ Switching patterns are shared with 180-degree and 90-degree phase switching within an antenna.
- ♦ Switching pattern length is 128.
- ♦ It is planned that 80 patterns (16 patterns for ACA and 64 patterns for 12m-Array) which are robust in time shift are selected from 128 patterns.
- ♦ 180-degree and 90-degree phase switching are nested. Switching base time of the 90-degree switching is a multiple of switching complete cycle of the 180-degree switching as shown in

Figure 1.

♦ The switching base time of the 180-degree switching is 125 μs. This indicates that the switching base time of the 90-degree switching is 16 ms (= 125 μs × 128 patterns).

We note that LO offset method is also implemented for the spurious cancellation and the sideband rejection (Napier 2007). The LO offset and the phase switching are exclusively used mutually.

2. Requirements for switching pattern in ACA

The modulation of the phase switching is performed at the 1st LO. This is common to ACA and 12m-Array. In addition, the ACA and the 12m-Array are sometimes combined and operated as single interferometer for high accuracy calibration. Thus, the specifications of the phase switching in the ACA are required to be identical with those of the 12m-Array. However, all of 128 patterns are not applicable to the ACA. ACA Correlator adopts FX architecture, and the switching base time is required to be a multiple of internal FFT operation interval (= 250 μs = 1,000,000 samples ÷ 4 Gsps). Since there are only 16 antennas in the ACA, a pattern length of 128 is not necessary. A pattern length of 16 or 32 (= 16 antennas × 1 or 2) is enough to choose switching patterns whose switching complete cycle is as short as possible and switching pattern is robust in time shift. By taking these restrictions into consideration, switching patterns for the ACA shall be satisfied with the following conditions:

♦ A pattern repeats twice or four times so that effective switching base time becomes 250 μs (= 125 μs × 2 consecutive patterns) or 500 μs (= 125 μs × 4 consecutive patterns).

♦ The switching pattern length is 32 (= 16 × 2 consecutive patterns), 64 (= 32 × 2 consecutive patterns or 16 × 4 consecutive patterns) or 128 (= 32 × 4 consecutive patterns) so that effective switching complete cycle becomes 16 or 32.

3. Selection of Walsh functions for ACA

3.1. Generation of Walsh functions

At first, Walsh functions of 128 patterns in length are generated in the natural or Paley order. These Walsh functions are conventionally written as PAL(n,t), which has the natural-order number n (hereafter, PAL index) and the time t between 0 and switching complete cycle. The product of two Walsh functions is another Walsh function. The PAL index of the generated Walsh function is given by modulo-2 addition of the binary PAL index of the component Walsh functions. Thus, PAL(n,t) can be generated as a product of Rademacher functions R(m,t). The following equation shows an example of the generation. Rademacher functions R(m,t) are simply square waves, where the half period of the square wave is (switching complete cycle)/2^m (m=0,1,2,…) (see Thompson et al. 2001).

$$\mathrm{PAL}(11=[1011]_2,t)=\mathrm{PAL}(8=[1000]_2,t)\cdot\mathrm{PAL}(2=[0010]_2,t)\cdot\mathrm{PAL}(1=[0001]_2,t)$$
$$=\mathrm{R}(4,t)\cdot\mathrm{R}(2,t)\cdot\mathrm{R}(1,t)$$

* $[]_2$ indicates binary number. Binary number $[1011]_2$ is divided into $[1000]_2$, $[0010]_2$ and $[0001]_2$ by modulo-2 addition.

Walsh functions are also given in order of number of zero-crossings within switching complete cycle; WAL(k,t), where k (hereafter, WAL index) indicates the number of zero-crossings (MEMO537).

After the generation of the Walsh functions, we have searched for the Walsh functions which are satisfied with the requirements for the phase switching in ACA. Table 1 shows all of the Walsh functions of 128 patterns in length, and the following four groups are candidates.

♦ Group-A (⟨effective switching base time = 250 μs⟩ × ⟨effective pattern length = 32 patterns⟩)

This is a group of Walsh functions whose effective switching base time is 250 μs (= 125 μs × 2 consecutive patterns) and effective pattern length is 32 (= 128/2 ÷ 2 consecutive patterns). We adopt 32 patterns in length, which is twice the number of ACA antennas, so as to select 16 functions which are robust in time shift. These Walsh functions are shown by hatches in red, orange, yellow and blue in Table 1. In this case, switching complete cycle of the 180-degree phase switching becomes (125 μs × 2) × (128/2 patterns ÷ 2) = 8 ms. Although the completion cycle of the 180-degree phase switching completes is 8 ms, the switching base time of 90-degree switching is always 16 ms (= 125 μs × 128 patterns) because of compatibility with the 12m-Array. Since switching patterns are identical between the 90-degree and 180-degree phase switching, switching complete cycle of the 90-degree phase switching becomes (16 ms × 2) × (128/2 patterns ÷ 2) = 1,024 ms.

♦ Group-B (⟨effective switching base time = 250 μs⟩ × ⟨effective pattern length = 16 patterns⟩)

This is a subset of Group A and gives high priority to short switching complete cycle. This group is shown by hatches in red and yellow. Its effective switching base time is same as that of Group A and its effective pattern length is 16 (= 128/4 ÷ 2 consecutive patterns). In this case, since the effective pattern length is shorter than that of Group A, switching complete cycle can effectively become shorter. They are (125 μs × 2) × (128/4 patterns ÷ 2) = 4 ms and (16 ms × 2) × (128/4 patterns ÷ 2) = 512 ms for the 180-degre and 90-degree phase switching, respectively.

♦ Group-C (⟨effective switching base time = 500 μs⟩ × ⟨effective pattern length = 32 patterns⟩)

This group consists of Walsh functions which have four consecutive patterns and complete their cycle in a pattern length of 128. They are shown by hatches in red, orange and green in Table 1. Switching complete cycles of the 180-degree and 90-degree phase switching are (125 μs × 4) × (128 patterns ÷ 4) = 16 ms and (16 ms × 4) × (128 patterns ÷ 4) = 2048 ms, respectively. With longer switching base time than those of Group-A and -B, it is expected that time shift between modulation and demodulation less impacts on phase switching performance. However, its switching complete cycle becomes longer than those of Group-A and -B.

♦ **Group-D (⟨effective switching base time = 500 μs⟩ × ⟨effective pattern length = 16 patterns⟩)**

This is a subset of Group C and gives high priority to short switching complete cycle. This group achieves shorter switching complete cycle than Group D by reducing effective switching pattern length from 32 to 16. These Walsh functions are shown by hatches in red and orange in Table 1. Switching complete cycle of the 180-degree and 90-degree switching are (125 μs × 4) × (64 patterns ÷ 4) = 8 ms and (16 ms × 4) × (64 patterns ÷ 4) = 1,024 ms, respectively.

We also attach ASCII format data files of these groups at the end of this PDF file. In these files, Walsh function amplitude of +1 and -1 are represented by +1 and 0, respectively, in order to save space. Walsh functions are arranged with positive phasing in WAL order, as suggested in Emerson (2006).

The PAL indexes of the available Walsh functions for the ACA are even and less than 63. This can be explained by the characteristics of Rademacher functions.
When a PAL index is 64 or more, Rademacher function R(7,t) is always used for the generation of the Walsh functions. Since the base time of R(7,t) is 1, the minimum base time of the generated Walsh functions is 1 and this is inconsistent with the first requirement in the ACA. On the other hand, when PAL index is less than 64, the base time of used Rademacher functions is 2^n (n=1,2,3,4,5,6) and a pattern always repeats twice.
When a PAL index is odd, Rademacher function R(1,t) is always used to generate the Walsh functions. Since R(1,t) consists of 64 consecutive “+1” and 64 consecutive “-1”, the first half and the latter half become opposite signs each other. Thus, switching pattern always completes in a length of 128 (green hatches of Group-C). On the other hand, Rademacher functions whose base time is 2n (n=0,1,2,3,4,5) are used to generate the Walsh functions of even PAL index. Since these Rademacher functions always complete their patterns in 64 patterns, the same patterns as the first half repeat in the latter half. (Group-A and -D)

3.2. Sensitivity loss and RSS crosstalk power

We have also estimated the following sensitivity loss and crosstalk power of the available Walsh functions for ACA as MEMO537 does:

- ♦ Sensitivity loss with 1% time shift between modulation and demodulation of an identical Walsh function. We additionally estimate averaged sensitivity loss between two Walsh functions, which involves 1% time shift between modulation and demodulation.
- ♦ Root-sum-of squares (RSS) crosstalk power with 1% time shift between two different Walsh functions.

In these estimations, we take only 180-degree phase switching into consideration. Since switching

base time of 90-degree phase switching is 16 ms and larger than that of 180-degree phase switching (250 μs or 500 μs), sensitivity loss and crosstalk caused by the 90-degree phase switching are expected to be smaller than those of the 180-degree phase switching by a factor of 64 (= 16 ms ÷ 250 μs) or 32 (= 16 ms ÷ 500 μs)

3.2.1. **Sensitivity loss by phase switching in ACA Correlator**

The ACA Correlator performs 1,048,576-point FFT every 250 μs. Since sampling frequency of ALMA digitizer is 4 GHz, the FFT lacks 48,576 data and the blank is filled with data of the next FFT segment (Kamazaki et al. 2006). If switching status changes between two consecutive FFT segments, the overlap of the FFT segments causes inconsistency between modulation and demodulation at the overlapped ranges as shown in Figure 2, which inconsistency is effectively identical with about 5 % time shift between modulation and demodulation. Thus, the FFT segment overlap introduces switching status change within a FFT segment, indicating that observation data are multiplied with a window function corresponding to the switching status in the time domain. In the frequency domain, they are convolved with a Fourier transform product of the switching status. When switching status does not change within a FFT segment, a window function becomes a constant value and there is no impact on observation data. However, with status change, the window function becomes a rectangle and the convolution of the function introduces sensitivity loss and frequency profile broadening to observation data.

We have calculated the sensitivity loss and the frequency profile broadening introduced by the FFT segment overlap in the ACA Correlator every pair of switching status. We assume that the overlap length is a constant of 10 % corresponding to 12.5 μs (= 50,000 samples) for the simplicity, although the length strictly depends on delay compensation. We also have estimated them including 1 % time shift (= 1.25 μs = 5,000 samples) between modulation and demodulation as MEMO 537 adopts. In the case of the ACA Correlator, the demodulation is conducted after FFT operations by the unit of a FFT segment and it is impossible to shift the demodulation timing by 1 %. Thus, we have shifted FFT segments before the FFT operations by 5,000 samples, which correspond to 1 % time shift, instead of shifting the demodulation timing.

♦ **Pair-α (p_i = +1 & p_j = +1, switching base time = 250 μs, no time shift)**

Switching status of two inputs does not change within FFT segments (see Figure 3a). Both of FFT products of the two switching status functions are δ functions and hence their multiplication is also δ function (see Figure 3c). Thus, neither sensitivity loss nor frequency profile broadening occurs in this case.

♦ **Pair-β (p_i = +1→-1 & p_j = +1, switching base time = 250 μs, no time shift)**

This is a case that switching status of an input does not change within a FFT segment but the other's status changes (see Figure 4a). This occurs in the case of cross correlation only. However, this does

not occur in the case of cross polarization of zero baselines in ALMA, because its dual polarization receivers adopt common LO signal between dual polarizations and their switching statuses are always identical. FFT product of the constant status function is δ function and that of the other becomes sinc like function as shown in Figure 4b. Their correlation multiplication also results in δ function and there is no impact on frequency response profile. However, some amount of power, which corresponds to extended components of the sinc like function in the frequency domain, are lost by the correlation multiplication because of no correlation and peak amplitude of the correlation result becomes lower than 1.0.

♦ **Pair-γ (p_i = +1→-1 & p_j = +1→-1, switching base time = 250 μs, no time shift)**

Switching status changes within both FFT segments (see Figure 5a). Their FFT products becomes sinc like functions as in the case of Pair-β, and their correlation multiplication results in sinc squared like function as shown in Figure 5b. Thus, peak amplitude becomes lower than 1.0 and frequency response profile becomes broadened in the frequency domain. Different from the case of Pair-β, the decreased power at the peak is not lost by the correlation multiplication but is distributed in the frequency domain (see Figure 5c). We can recover the sensitivity by spectral integration as shown in Table 2 and Table 3. Strictly to say, there is slight delay error in residual delay compensation because of different frequency, however this can be negligible in ACA. Hereafter, we refer the broadened components as “sensitivity leakage”.

We summarize peak amplitude, sensitivity leakage and sensitivity loss of above three cases (Pair-α, -β and -γ) in Table 2 and Table 3. They show results in the case that switching base time is 250 μs and 500 μs and both of them include effect of the 5 % FFT segment overlap. Since the sensitivity is recovered by spectral integration in Pair-γ as previously mentioned, peak amplitude, sensitivity leakage and sensitivity loss are written every spectral averaging factor up to 1024 frequency channels, which is the maximum value of the ACA Correlator. We also list values additionally including 1.0 % time shift for the comparison with MEMO537. Since additional 1.0 % time shift increases width of inconsistent switching status, its FFT product becomes slightly different from that of switching status function without the time shift and sensitivity leakage and loss increase.

3.2.2. **Sensitivity leakage and loss**

We estimate sensitivity leakage and loss of the Walsh functions which are selected as candidates for phase switching patterns of ACA in Section 3.1. Concretely, sensitivity leakage and loss at each switching status pair, which are calculated in Section 3.2.1, are averaged over switching complete cycle every pair of Walsh functions hatched in Table 1. Their results about pairs of identical Walsh functions are plotted in Figure 6 and Figure 7. We also show average sensitivity leakage and loss, which averages the sensitivity leakage and loss about all pairs every Walsh function, in Figure 8 and

Figure 9. For example, in the case of the WAL index of 1 of Group-C, the average sensitivity leakage and loss are calculated by averaging sensitivity leakages and losses of WAL index pairs (1,0), (1,1), …, (1,30) and (1,31), respectively. The plots show only Group-A and -C results, because Group-B and -D are subsets of Group-A and -C, respectively. The sensitivity leakage depends on spectral integration as mentioned in Section 3.2.1 and hence, there are two plots in each group. One plot shows results without averaging in the frequency domain. In the other plot, spectral averaging is performed by 8 frequency channels, which correspond to 30.5 kHz and 0.040 km/s at 230 GHz.

Figure 6 and Figure 7 show that sensitivity leakage becomes larger as WAL index increases. This is natural because sensitivity leakage occurs around zero-crossing points of Walsh functions and larger WAL index indicates more frequent zero-crossings. They also show that the sensitivity leakage can be decreased by adopting longer switching base time and/or spectral integration in the frequency domain as we expect. Sensitivity loss is zero in Figure 6 and Figure 7, because no sensitivity loss occurs in the case of auto correlation as shown in Pair-α and Pair-γ of Table 2 and Table 3.

Figure 8 and Figure 9 also show larger sensitivity leakage as WAL index increases and smaller sensitivity leakage by longer switching base time and/or spectral integration. These are the same reason as Figure 6 and Figure 7. However, sensitivity loss is constant as WAL index increases. This is because the number of Pair-β is constant among candidates for the ACA Walsh functions.

3.2.3. **RSS crosstalk power**

We also estimate RSS crosstalk power with same method as MEMO537. At first, we estimate crosstalk power every pair of the Walsh functions with 1 % time shift between them. In this calculation, we ignore components contributed from different frequency channels by the frequency profile expansion of Pair-γ for the simplicity. And then, RSS crosstalk power is calculated every Walsh function by conducting root-sum-of square of the estimated crosstalk power. These results are plotted in Figure 10 and Figure 11. We show only Group-A and -C results same as Section 3.2.2.

Figure 10 and Figure 11 show that the RSS crosstalk power can be decreased by adopting longer switching base time, because longer switching base time bring about less decrease from 1.0 in peak amplitude (see Table 2 and Table 3).

In the case of the combined array, since 80 of 128 Walsh functions are used and 64-antenna Correlator process all of baselines, the RSS crosstalk power are necessary to be estimated from 128 Walsh functions with the method in MEMO537.

3.3. Selection of Walsh functions

For the case of ACA only, our simulation results suggest that WAL index of the available Walsh functions shall be smaller in the viewpoint of the sensitivity leakage. They also suggest that WAL index around 16 and 48 for Group-A and around 8 and 24 for Group-C shall be avoided because of large RSS crosstalk power. On the other hand, for the case of the combined array, the sensitivity loss

and the crosstalk power become smaller in the range of WAL index of 63 or less as the WAL index becomes smaller (see Figure 4 & 5 in MEMO537). In addition, the sensitivity loss can not be recovered and spectral integration in the frequency domain is necessary to reduce the sensitivity leakage, although the crosstalk power is expected to be reduced by cross correlation because of incoherency. Thus, we think that lower sensitivity leakage and loss is more important than lower crosstalk power. By taking them into consideration, WAL indexes from 0 to 15 of Group-C (effective switching base time = 500 μs, effective pattern length = 32 patterns) are preferable to Walsh functions used in ACA. With this selected Walsh functions, the sensitivity leakage and loss can achieve 2.5 % or less and 0 % in the case of 1% time shift between modulation and demodulation of an identical Walsh function without spectral integration in the frequency domain, respectively. The averaged sensitivity leakage and loss over the combination of two Walsh functions are 1.3 % or less and 1.3 % or less in the same case, respectively. The RSS crosstalk power can achieve 1.2 % or less in the case of 1 % time shift between two different Walsh functions without spectral integration in the frequency domain, respectively.

References

Emerson, D.T., Walsh Function Demodulation in the Presence of Timing Errors, leading to Signal Loss and Crosstalk, ALMA Memo 537, 2005

Emerson, D.T., Walsh Function Definition for ALMA, ALMA Memo 565, 2006

Kamazaki, T., Chikada, Y. and Okumura, S.K., ACA Correlator Design Description, CORL-62.00.00.00-012-A-DSN, 2006

Napier, P., ALMA Use of LO Offsetting for Spurious Signal Suppression and Sideband Rejection, SYSE-80.04.00.00-018-A-DSN, 2007

Thompson, A.R., Moran, J.M. and Swenson, G.W. Jr., Interferometry and Synthesis in Radio Astronomy, Second Edition, John Wiley & Sons, 2001: ISBN 0-471-25492-4.

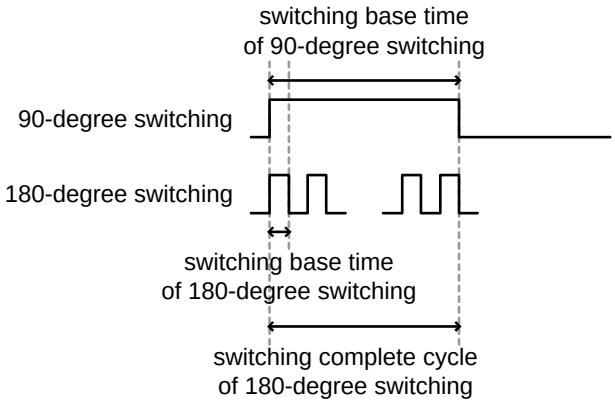

Figure 1 90-degree and 180-degree phase switching

180-degree and 90-degree phase switching are nested in ALMA. Switching base time of the 90-degree switching is a multiple of the switching complete cycle of the 180-degree switching.

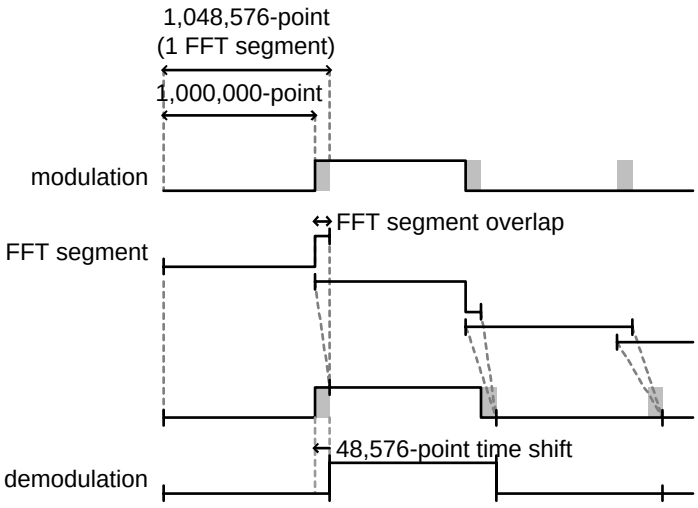

Figure 2 FFT segment overlap in the ACA Correlator

Since a FFT segment makes up for 48.576 data with the data of next FFT segment, switching status change between the two segments causes inconsistency between modulation and demodulation at the overlapped region. This effect is seen as 48,576-point time shift of the modulation as shown by dashed-dotted line.

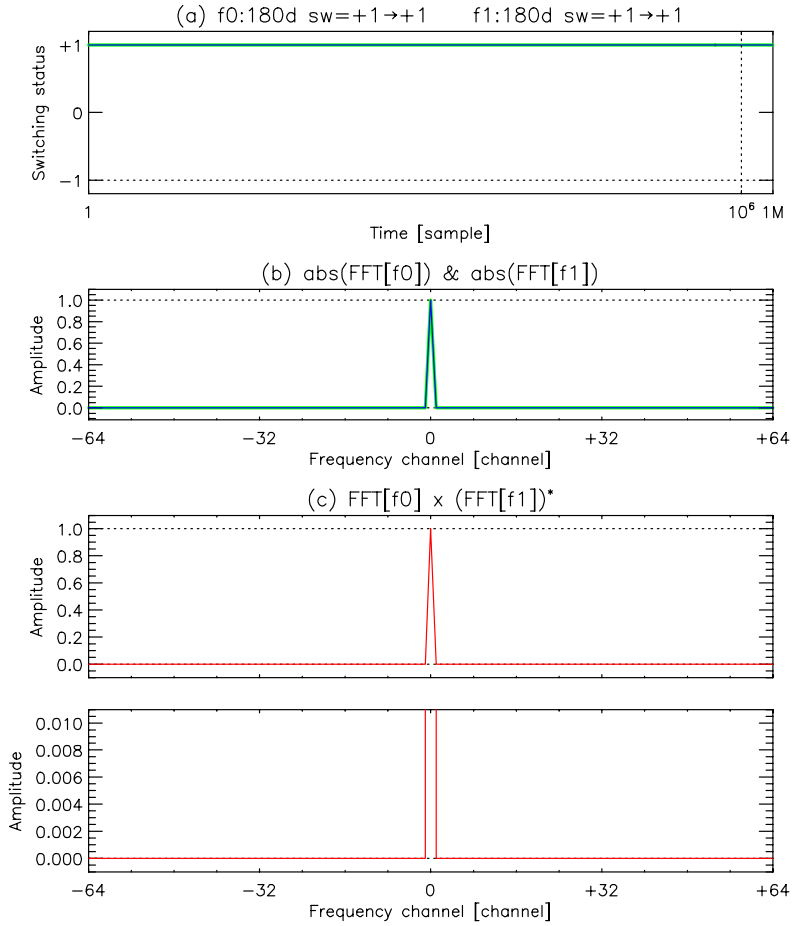

Figure 3 Sensitivity loss and frequency profile broadening in the case of no switching status change within a FFT segment (switching base time = 250 μs, no time shift)

(a) Blue and green lines show phase switching statuses. (b) Blue and green lines show FFT products of the phase switching statuses in (a). (c) Red lines show correlation multiplication results of the two FFT products in the upper figure. Lower figure is a close-up of the upper one in the Y-axis.

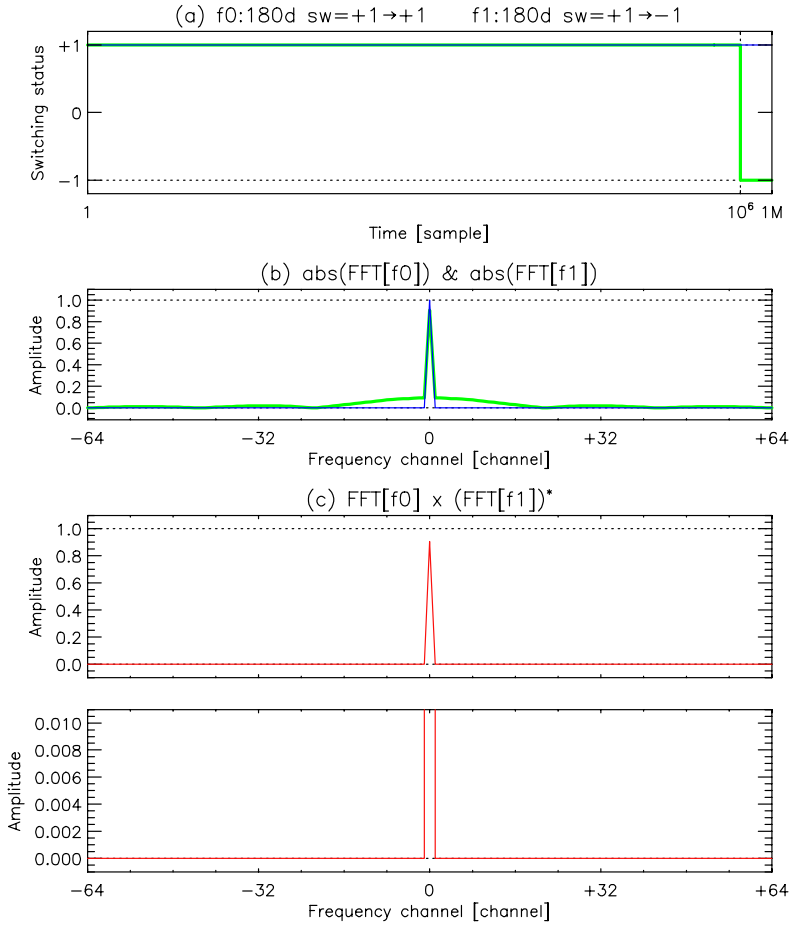

Figure 4 Sensitivity loss and frequency profile broadening in the case of two inputs with and without switching status changes within a FFT segment (switching base time = 250 μs, no time shift)

(a) Blue and green lines shows phase switching statuses. (b) Blue and green lines show FFT products of the phase switching statuses in (a). (c) Red lines show a correlation multiplication result of the two FFT products in the upper figure. Lower figure is a close-up of the upper one in the Y-axis.

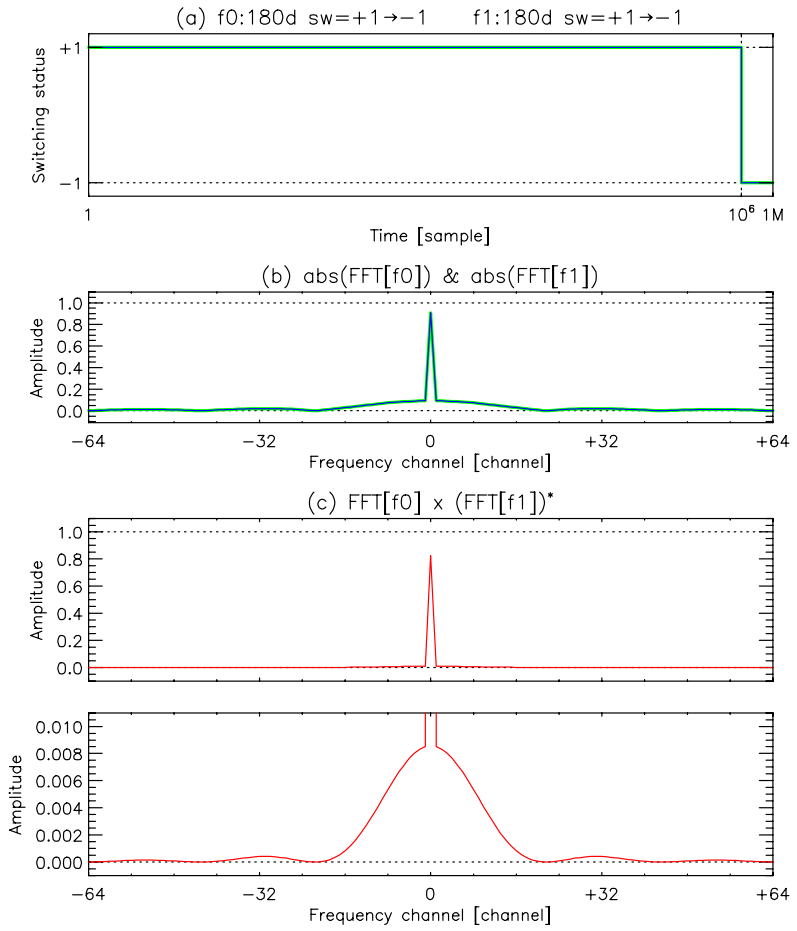

Figure 5 Sensitivity loss and frequency profile broadening in the case of two inputs with switching status changes within a FFT segment (switching base time = 250 μs, no time shift)

(a) Blue and green lines show phase switching statuses. (b) Blue and green lines show FFT products of the phase switching statuses in (a). (c) Red lines show correlation multiplication results of the two FFT products in the upper figure. Lower figure is a close-up of the upper one in the Y-axis.

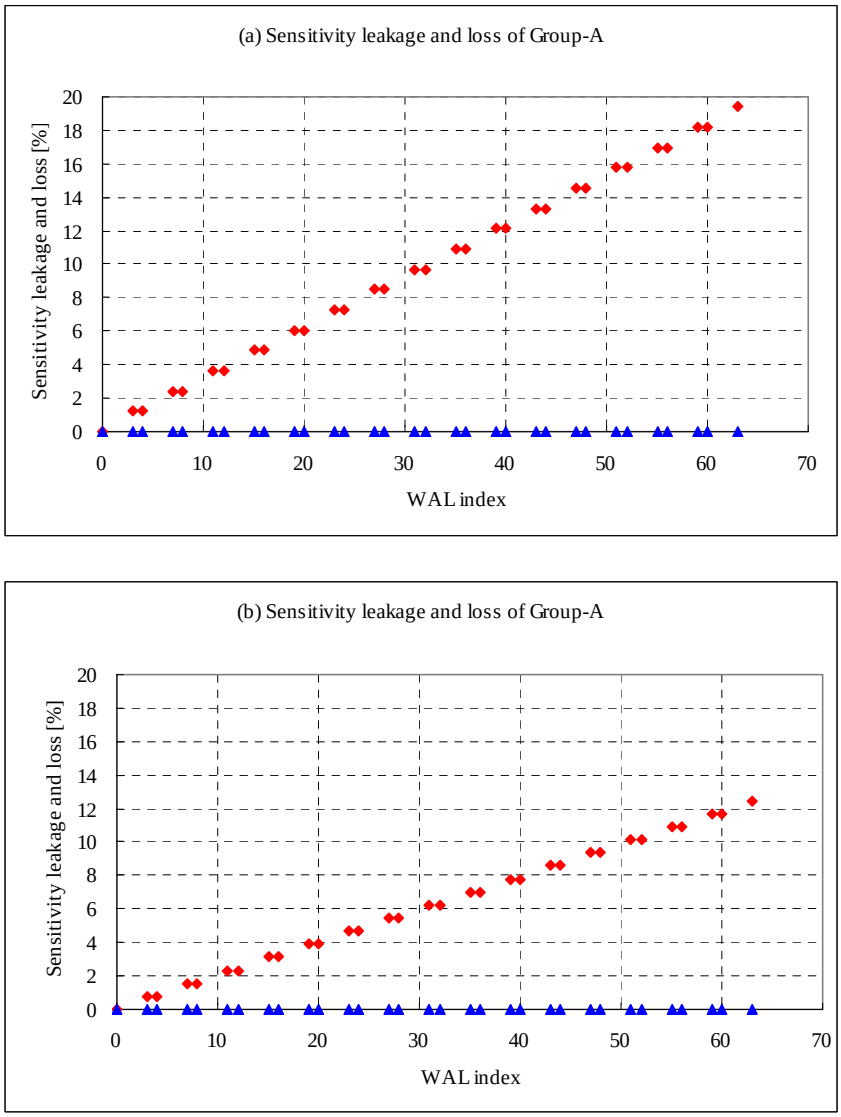

Figure 6 Sensitivity leakage and loss of Group-A with 5% FFT segment overlap and 1% time shift with an identical Walsh function

(a) Sensitivity leakage (red diamonds) and loss (blue triangles) without spectral integration. (b) Sensitivity leakage (red diamonds) and loss (blue triangles) with spectral integration by 8 frequency channels.

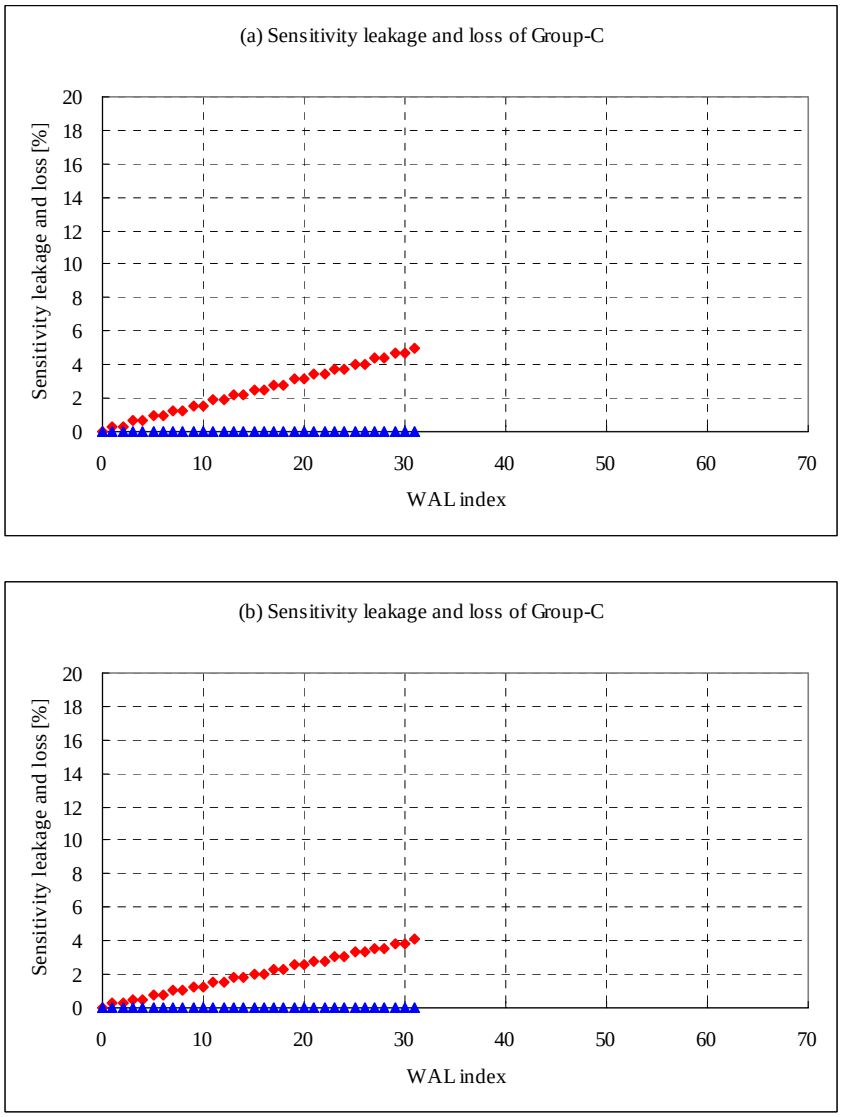

Figure 7 Sensitivity leakage and loss of Group-C with 5% FFT segment overlap and 1% time shift with an identical Walsh function

(a) Sensitivity leakage (red diamonds) and loss (blue triangles) without spectral integration. (b) Sensitivity leakage (red diamonds) and loss (blue triangles) with spectral integration by 8 frequency channels.

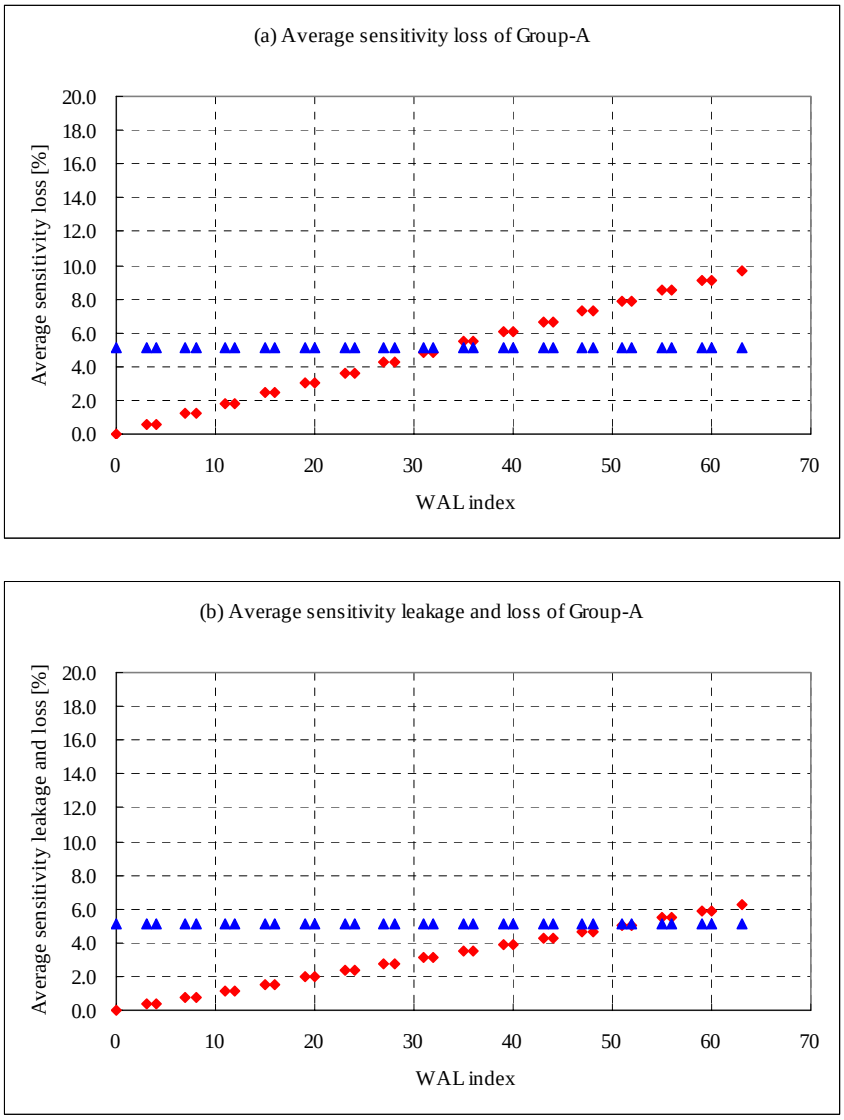

Figure 8 Average sensitivity leakage and loss of Group-A with 5% FFT segment overlap and 1% time shift with two Walsh functions

(a) Average sensitivity leakage (red diamonds) and loss (blue triangles) without spectral integration. Black squares show the total of them. (b) Average sensitivity leakage (red diamonds) and loss (blue triangles) with spectral integration by 8 frequency channels. Black squares show the total of them.

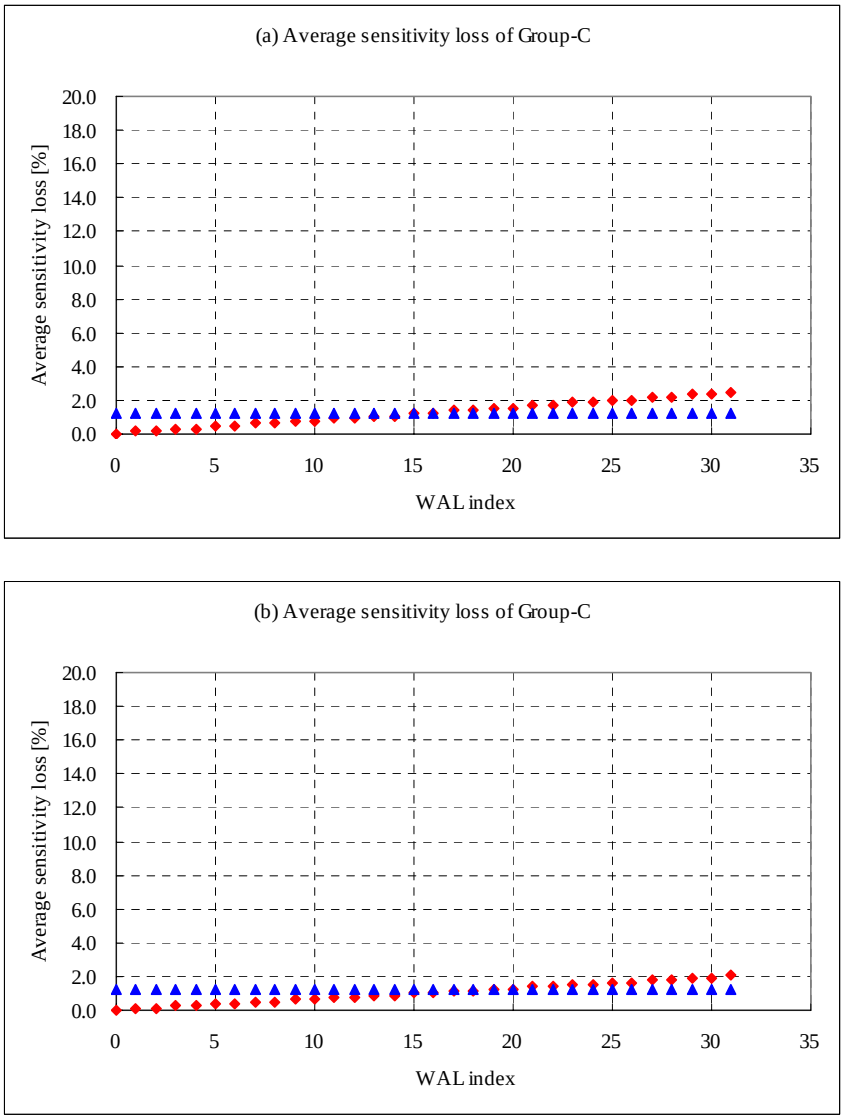

Figure 9 Average sensitivity leakage and loss of Group-C with 5% FFT segment overlap and 1% time shift with two Walsh functions

(a) Average sensitivity leakage (red diamonds) and loss (blue triangles) without spectral integration. Black squares show the total of them. (b) Average sensitivity leakage (red diamonds) and loss (blue triangles) with spectral integration by 8 frequency channels. Black squares show the total of them.

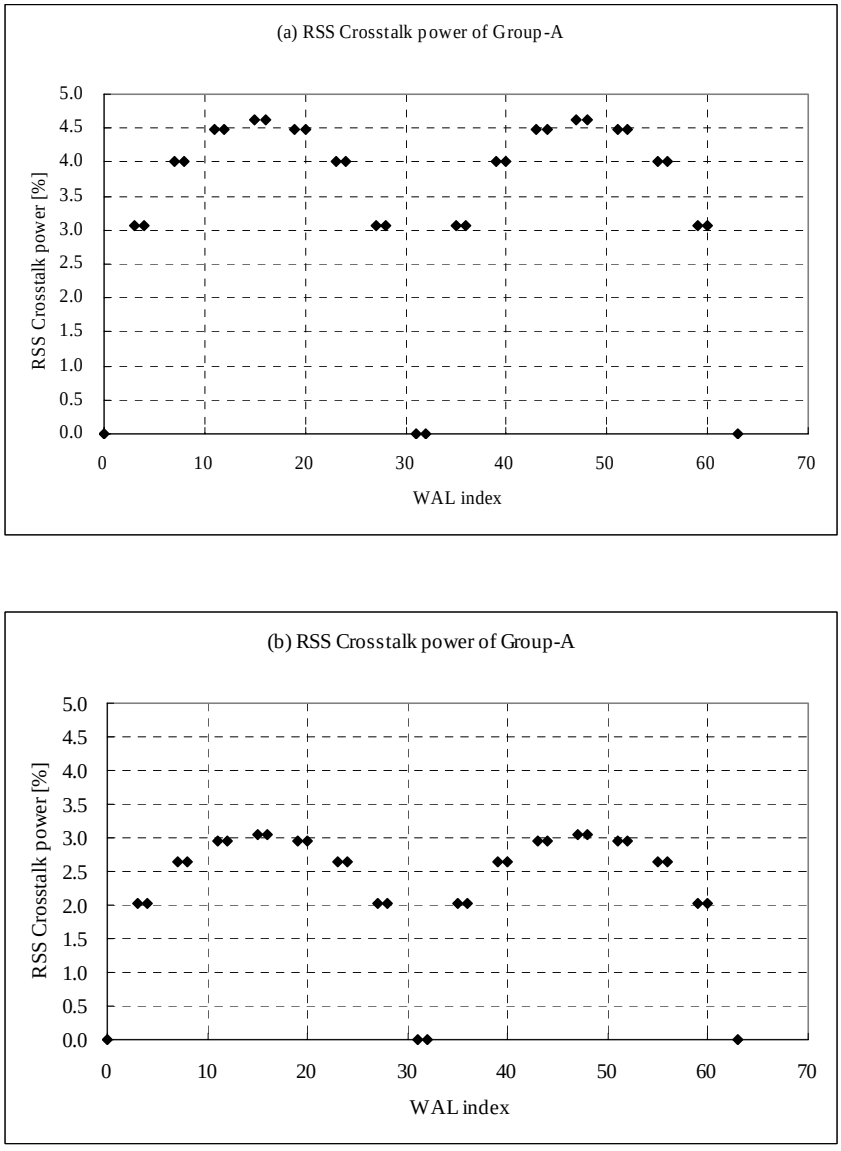

Figure 10 RSS Crosstalk power of Group-A with 5% FFT segment overlap and 1% time shift between two different Walsh functions (Group-A)

(a) RSS crosstalk power without spectral integration. (b) RSS crosstalk power with spectral integration by 8 frequency channels.

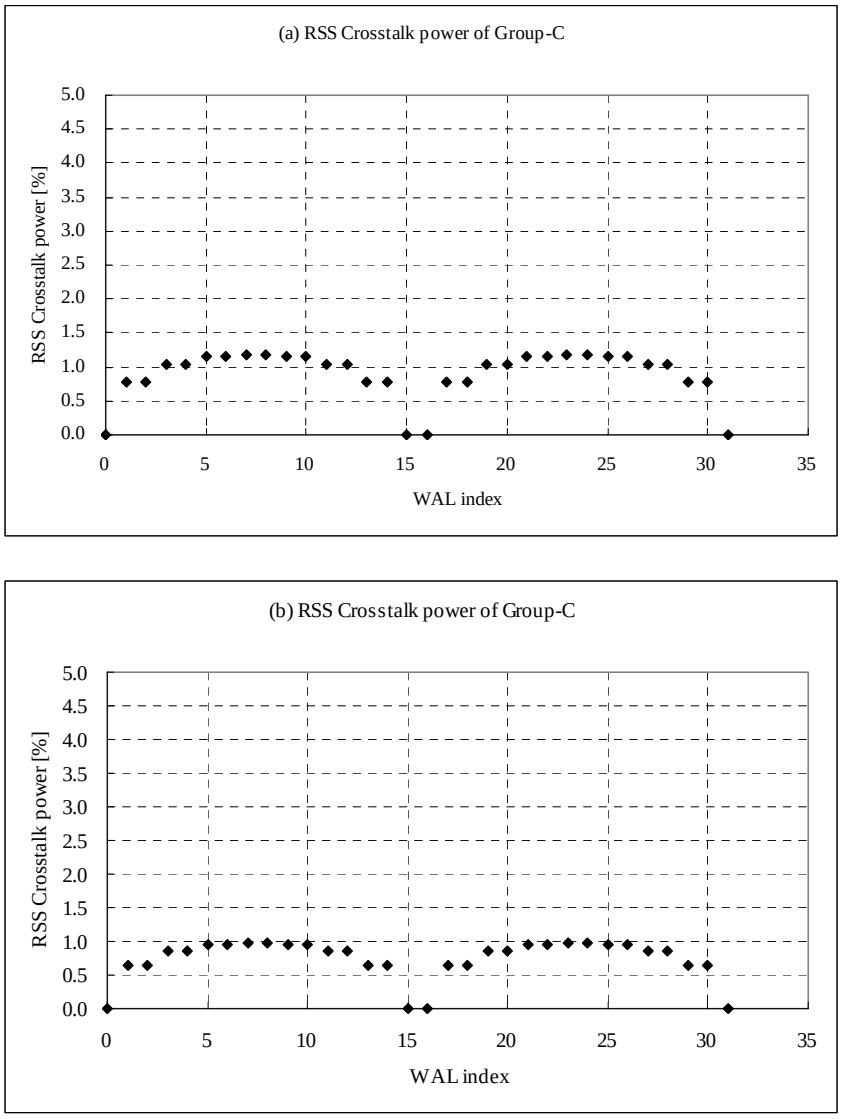

Figure 11 RSS Crosstalk power of Group-C with 5% FFT segment overlap and 1% time shift between two different Walsh functions (Group-C)

(a) RSS crosstalk power without spectral integration. (b) RSS crosstalk power with spectral integration by 8 frequency channels.

Table 1 Walsh functions of 128 patterns in length

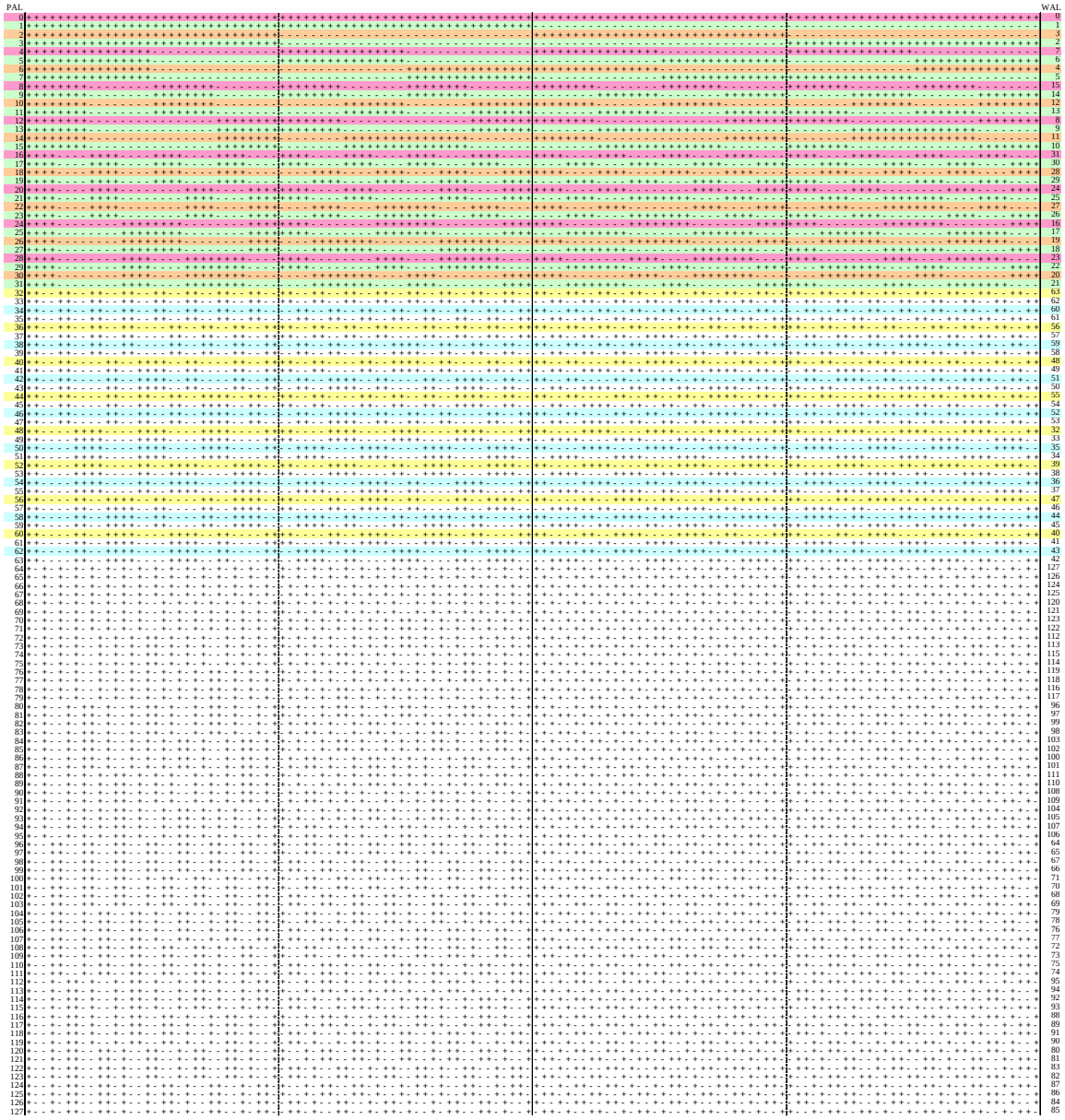

Group-A: red, orange, yellow and blue hatches

Group-B: red and yellow hatches

Group-C: red, orange and green hatches

Group-D: red and orange hatches

Table 2 Peak amplitude and sensitivity loss of every switching status pair
(switching base time = 250 μs)

Pair	Spectral integration [channel]	No time shift at demodulation			1.0 % time shift at demodulation (*1)			1.0% time shift at demodulation of only an input (*2)		
		Peak amplitude	Sensitivity		Peak amplitude	Sensitivity		Peak amplitude	Sensitivity	
			leakage	loss		leakage	loss		leakage	loss
α	---	1.000	0.000	0.000	1.000	0.000	0.000	1.000	0.000	0.000
β	---	0.907	0.000	0.093	0.898	0.000	0.102	0.898	0.000	0.102
γ	1	0.823	0.177	0.000	0.806	0.194	0.000	0.815	0.181	0.004
γ	2	0.832	0.168	0.000	0.816	0.184	0.000	0.824	0.172	0.004
γ	4	0.849	0.151	0.000	0.837	0.163	0.000	0.843	0.153	0.004
γ	8	0.881	0.119	0.000	0.875	0.125	0.000	0.878	0.118	0.004
γ	16	0.933	0.067	0.000	0.936	0.064	0.000	0.934	0.062	0.004
γ	32	0.979	0.021	0.000	0.979	0.021	0.000	0.978	0.018	0.004
γ	64	0.987	0.013	0.000	0.988	0.012	0.000	0.986	0.010	0.004
γ	128	0.994	0.006	0.000	0.993	0.007	0.000	0.991	0.005	0.004
γ	256	0.997	0.003	0.000	0.997	0.003	0.000	0.994	0.002	0.004
γ	512	0.998	0.002	0.000	0.998	0.002	0.000	0.995	0.001	0.004
γ	1024	0.999	0.001	0.000	0.999	0.001	0.000	0.996	0.000	0.004

*All pairs include 5 % FFT segment overlap.

*1 1.0 % time shift occurs at demodulation in both of two inputs.

*2 1.0 % time shift at demodulation occurs in an input only of two inputs. There is no time shift in the other input. This occurs only at cross correlation between different antennas.

Table 3 Peak amplitude and sensitivity loss of every switching pattern pair
(switching base time = 500 μs)

Pair	Spectral integration [channel]	No time shift at demodulation			1.0% time shift at demodulation (*1)			1.0% time shift at demodulation of only an input (*2)		
		Peak amplitude	Sensitivity		Peak amplitude	Sensitivity		Peak amplitude	Sensitivity	
			leakage	loss		leakage	loss		leakage	loss
α	---	1.000	0.000	0.000	1.000	0.000	0.000	1.000	0.000	0.000
β	---	0.954	0.000	0.046	0.949	0.000	0.051	0.949	0.000	0.051
γ	1	0.909	0.091	0.000	0.900	0.100	0.000	0.905	0.093	0.002
γ	2	0.912	0.088	0.000	0.903	0.097	0.000	0.907	0.091	0.002
γ	4	0.916	0.084	0.000	0.908	0.092	0.000	0.912	0.086	0.002
γ	8	0.924	0.076	0.000	0.918	0.082	0.000	0.921	0.077	0.002
γ	16	0.940	0.060	0.000	0.938	0.062	0.000	0.939	0.059	0.002
γ	32	0.967	0.033	0.000	0.968	0.032	0.000	0.967	0.031	0.002
γ	64	0.990	0.010	0.000	0.990	0.010	0.000	0.989	0.009	0.002
γ	128	0.993	0.007	0.000	0.994	0.006	0.000	0.993	0.005	0.002
γ	256	0.997	0.003	0.000	0.997	0.003	0.000	0.996	0.002	0.002
γ	512	0.998	0.002	0.000	0.998	0.002	0.000	0.997	0.001	0.002
γ	1024	0.999	0.001	0.000	0.999	0.001	0.000	0.997	0.001	0.002

*All pairs include 5 % FFT segment overlap.

*1 1.0 % time shift occurs at demodulation in both of two inputs.

*2 1.0 % time shift at demodulation occurs in an input only of two inputs. There is no time shift in the other input. This occurs only at cross correlation between different antennas.